Anisotropic enhancement of lower critical field in ultraclean crystals of spin-triplet superconductor candidate UTe₂

K. Ishihara [1,*] M. Kobayashi,[1] K. Imamura [1] M. Konczykowski [2] H. Sakai [3] P. Opletal,[3] Y. Tokiwa,[3] Y. Haga [3]
K. Hashimoto [1] and T. Shibauchi [1,†]

[1]*Department of Advanced Materials Science, University of Tokyo, Kashiwa, Chiba 277-8561, Japan*
[2]*Laboratoire des Solides Irradiés, CEA/DRF/IRAMIS, Ecole Polytechnique, CNRS, Institut Polytechnique de Paris,
F-91128 Palaiseau, France*
[3]*Advanced Science Research Center, Japan Atomic Energy Agency, Tokai, Ibaraki 319-1195, Japan*

The paramagnetic spin-triplet superconductor candidate UTe₂ has attracted significant attention because of its exotic superconducting properties including an extremely high upper critical field and possible chiral superconducting states. Recently, ultraclean single crystals of UTe₂ have become available, and thus measurements on these crystals are crucial to elucidate the intrinsic superconducting properties. Here, we report the thermodynamic critical field H_c, the lower critical field H_{c1}, and the upper critical field H_{c2} at low fields of these high-quality single crystals. From the comparison of the anisotropies in H_{c1} and H_{c2}, we find that the experimental H_{c1} values with the magnetic field along the b and c axes are anomalously enhanced, showing unusual low-temperature upturns. We propose an effect of the strong Ising-like ferromagnetic fluctuations on the vortex line energy as the origin of the anisotropic enhancement of H_{c1}.

The superconducting state of UTe₂ has been intensively investigated because of its putative spin-triplet nature with a paramagnetic normal state [1,2]. The spin-triplet pairing state induces an extremely high upper critical field (H_{c2}) beyond the Pauli limit [1,3] and multiple superconducting phases under hydrostatic pressure or magnetic field [4–9]. Furthermore, chiral spin-triplet states are discussed in scanning tunneling microscopy [10], polar Kerr effect [11], surface impedance [12], and penetration depth studies [13]. As for the pairing interactions, the anisotropic H_{c2} and reentrant superconductivity [3,14] suggest that ferromagnetic fluctuations are at play analogous to the ferromagnetic superconductors [15], which is supported by the nuclear magnetic resonance (NMR) and muon-spin rotation (μSR) measurements [16–18]. On the other hand, recent neutron-scattering studies revealed the presence of antiferromagnetic fluctuations related to superconductivity [19–21]. However, there is a different report on neutron-scattering data [22], and their interpretation is controversial. Thus, the nature of magnetic fluctuations and their relationship to superconductivity are still unclear.

What has complicated systematic understandings of the superconducting state in UTe₂ are the inhomogeneity of crystals and the presence of magnetic impurities. Single crystals

grown by the conventional chemical vapor transport method sometimes show double superconducting transitions likely induced by inhomogeneity [11,23,24] and a small increase in magnetic susceptibility at low temperatures, which reflects the presence of U vacancies acting as magnetic impurities [1,18,24–26]. Recently, Sakai *et al.* developed another crystal growth method called the molten salt flux (MSF) method and succeeded in obtaining high-quality single crystals of UTe₂ with a transition temperature $T_c = 2.1$ K, a residual resistivity ratio as high as 1000, and low magnetic impurity density [27]. In these ultraclean crystals, novel superconducting- and normal-state properties have been reported in addition to the observation of de Haas–van Alphen oscillations [9,28,29]. Therefore, measurements on the high-quality single crystals are crucial to clarify the superconducting nature in UTe₂.

In this study, we investigate the thermodynamic critical field (H_c), the lower critical field (H_{c1}), and the upper critical field (H_{c2}) in high-quality MSF single crystals. Regarding the Ginzburg-Landau (GL) theory, the anisotropies in H_{c1} and H_{c2} should be opposed because the critical fields satisfy $H_{c1}H_{c2} = H_c^2(\ln \kappa + 0.5)$, where κ is the GL parameter, and H_c is independent of field directions. In contrast, we find that the anisotropy of H_{c1} does not follow the expectations from that of H_{c2}. Quantitatively, the above GL relation holds for $\boldsymbol{H} \parallel \boldsymbol{a}$, while it is obviously violated for $\boldsymbol{H} \parallel \boldsymbol{b}$. Furthermore, H_{c1} for $\boldsymbol{H} \parallel \boldsymbol{b}$ and $\boldsymbol{H} \parallel \boldsymbol{c}$ show unusual upturns at low temperatures. To explain these anomalous behaviors of the critical fields, we propose an anisotropic enhancement of H_{c1} induced by the Ising-like ferromagnetic fluctuations in UTe₂.

High-quality single crystals are grown by the MSF method as described in Ref. [27]. Crystals #A1 and #A2 in this study are the same samples as crystal #A1 in Ref. [13] and crystal

*k.ishihara@edu.k.u-tokyo.ac.jp
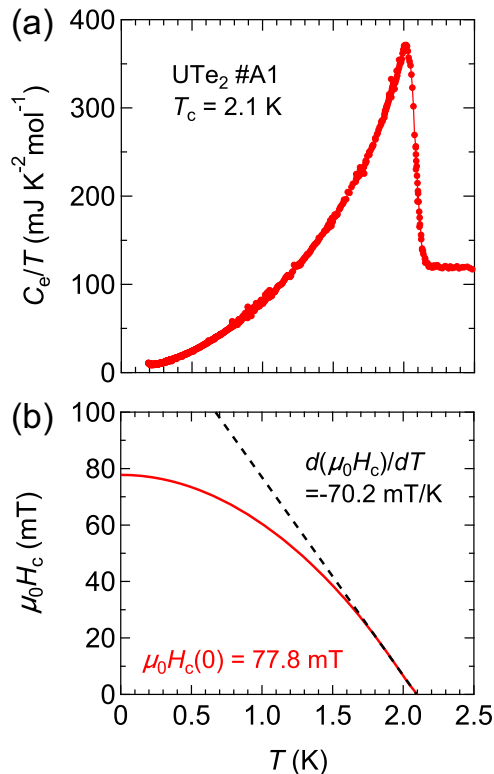†shibauchi@k.u-tokyo.ac.jp

FIG. 1. (a) Electronic specific heat C_e divided by temperature T as a function of temperature measured in crystal #A1. The phonon contributions are subtracted. (b) Temperature dependence of the thermodynamic critical field calculated from the specific-heat data. The black broken line represents the initial slope of H_c estimated near T_c.

#M7-1 in Ref. [27], respectively, and crystal #A3 for the H_{c2} measurement is picked up from the same batch with the crystal used in the de Haas–van Alphen experiments [29]. Crystals #A1 and #A2 have a cuboid shape with dimensions $455 \times 250 \times 95$ μm^3 and $1400 \times 285 \times 165$ μm^3, respectively. H_c is calculated from the specific heat measured by the long-relaxation method where a Cernox resistor is used as a thermometer, a heater, and a sample stage [30]. H_{c1} is measured by a miniature Hall-sensor array probe tailored in a GaAs/AlGaAs heterostructure [31–34]. The distance of neighboring sensors is 20 μm so that we can measure the local magnetic induction and the first flux penetration field H_p near crystal edges. H_{c2} is estimated from specific-heat data $C(T)$ near T_c measured in the physical property measurement system (Quantum Design). The same single-crystal piece appropriately shaped relative to the principal axes was used for all the field directions relative to the crystal orientation.

Figure 1(a) shows the temperature dependence of electronic specific heat C_e divided by temperature T of crystal #A1. A sharp peak at 2.1 K and a small residual value at low temperatures confirm that this crystal is ultraclean. H_c can be calculated via $H_c^2(T) = 2\mu_0 \int_T^{T_c} (S_n - S_{sc}) dT$, where μ_0 is the permeability of vacuum and S_{sc} and S_n are the electronic entropy in the superconducting and normal states, respectively, calculated from the electronic specific heat. The details of the calculation procedures are explained in the Supplemental Material [35]. The obtained $\mu_0 H_c(0) = 77.8$ mT shown in

Fig. 1(b) is higher than the reported value in a low-T_c crystal [36], reflecting the higher quality of our crystal.

Figure 2 represents external magnetic-field dependence of the local magnetic induction B_{edge} near the crystal edges of crystal #A1. The typical behaviors of the Hall resistance of the Hall-array probe near the crystal edges are shown in the insets in Fig. 2. The linear dependence at the low-field region originates from the finite distance between the Hall sensor and the crystal. By subtracting the linear function, we can derive the local magnetic induction B_{edge}. At lower fields, $B_{edge} = 0$ because of the Meissner state. As the magnetic field increases, the B_{edge} value deviates from zero at H_p depicted as black triangles in Fig. 2. We found that the H_p value does not depend on the crystal positions (see Supplemental Material), confirming that our measurements are free from surface pinning or geometrical barriers of superconducting vortices. Here, we note that H_p is lower than the bulk H_{c1} because of the demagnetization effect. The relation between H_p and H_{c1} has been precisely studied [37], and we can evaluate H_{c1} from H_p through

$$H_{c1} = \frac{H_p}{\tanh \sqrt{0.36 t/w}}, \quad (1)$$

where t and w are the sample thickness and width, respectively.

The obtained H_{c1}^i with the magnetic field along the i axis is shown in Fig. 3. Considering the usual relation

$$\mu_0 H_{c1} = \frac{\phi_0}{4\pi \lambda^2}(\ln \kappa + 0.5), \quad (2)$$

$H_{c1}(T)$ is expected to scale with the normalized superfluid density $\rho_s(T) \propto \lambda^{-2}(T)$ when the temperature dependence of the GL parameter, κ, is small. The black solid line in Fig. 3(a) is the normalized superfluid density for $\boldsymbol{H} \parallel \boldsymbol{a}$, $\rho_s^a = [\lambda_b^2(0)/\lambda_b^2(T) + \lambda_c^2(0)/\lambda_c^2(T)]/2$, calculated from the anisotropic penetration depth measurements [13]. It is obvious that H_{c1} and ρ_s^a show similar T dependence, confirming the consistency of H_{c1} and penetration depth measurements. On the other hand, the H_{c1} data along the b and c axes show an anomalous concave temperature dependence around 0.5 K, which is not detected in the penetration depth measurements. The origin of this unusual T dependence will be discussed later. We note that, although the absolute value of H_{c1}^c in crystal #A1 may have an estimation error of the demagnetization effect because of its platelike shape, we obtain very similar $H_{c1}^c(T)$ in another crystal, #A2 [Fig. 3(c)], confirming the correct estimation of H_{c1}^c values in these crystals.

First, we compare the anisotropies in H_{c1} and H_{c2}. As mentioned before, the GL theory implies that the anisotropies in these critical fields are opposite as long as we discuss the initial slope near T_c where the GL formalism is valid. Figure 4 depicts $H_{c2}^i(T)$ with the magnetic field along the i axis near $T_c = 2.1$ K. The slope of $H_{c2}(T)$ along the a axis significantly changes with decreasing temperature in the low-field region, which has been already reported in previous studies [8,38]. Focusing on the initial slope, we find the anisotropy of $H_{c2}^b > H_{c2}^a > H_{c2}^c$. In contrast, from the initial slope of H_{c1} data (see Fig. 3), we obtain the anisotropy $H_{c1}^c > H_{c1}^b > H_{c1}^a$, the order of which is not as expected from the anisotropy
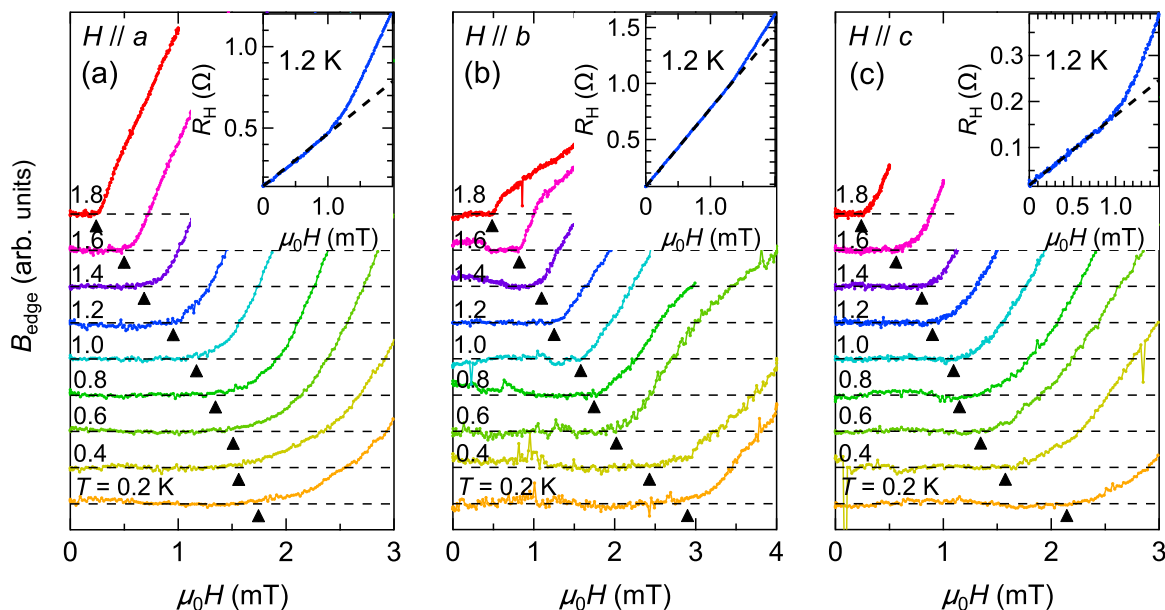
FIG. 2. (a)–(c) The insets show a typical magnetic-field dependence of the Hall resistivity near a crystal edge with the magnetic field along each crystallographic axis. The black broken line is the linear fitting of the data at the low-field region. The main panels show the local magnetic induction measured in crystal #A1 with the magnetic field along the a, b, and c axes, respectively. The black triangles are the first penetration field H_p. The data are shifted vertically for clarity, and the black broken lines show $B_{edge} = 0$ for each measurement temperature.

of H_{c2}. We note that, while the anisotropy in H_{c1} is similar to the previous study of global magnetization measurements in a lower-quality sample [36], the absolute values of H_{c1} in this study are considerably larger. This point is important to discuss the origin of the discrepancy between the anisotropies of H_{c1} and H_{c2} as described below.

To discuss possible origins of this apparent inconsistency in critical-field anisotropies, we calculate the lower critical field H_{c1}^{cal} expected from H_c and H_{c2} values via the following

GL relations:

$$H_{c2} = \sqrt{2}\kappa H_c, \qquad (3)$$

$$H_{c1}^{cal} = \frac{H_c}{\sqrt{2}\kappa}(\ln \kappa + 0.5). \qquad (4)$$

The results are shown in Fig. 3 as the black broken lines. We can clearly find in Fig. 3(a) that H_{c1}^{cal} along the a axis matches well with the experimental H_{c1} value, meaning that
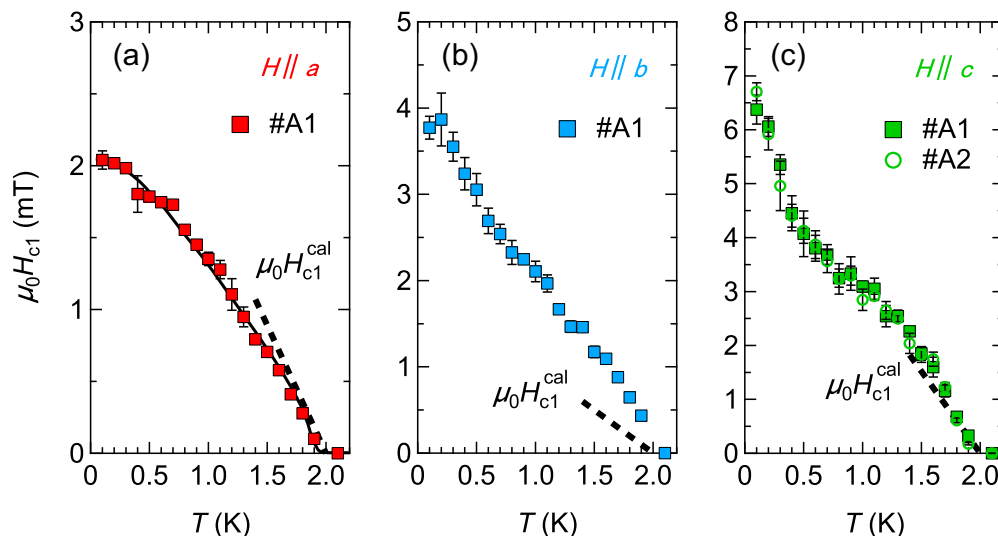

FIG. 3. (a)–(c) Lower critical field as a function of temperature with the magnetic field along a, b, and c axes, respectively, evaluated from Eq. (1). The black broken lines represent the initial slope of the lower critical field expected from the usual GL relations. The black solid line in (a) is obtained by multiplying the normalized superfluid density $[\lambda_b^2(0)/\lambda_b^2(T) + \lambda_c^2(0)/\lambda_c^2(T)]/2$ by a constant value calculated from the temperature dependence of the anisotropic penetration depth measurements [13]. The filled squares and open circles are the data obtained in crystals #A1 and #A2, respectively.
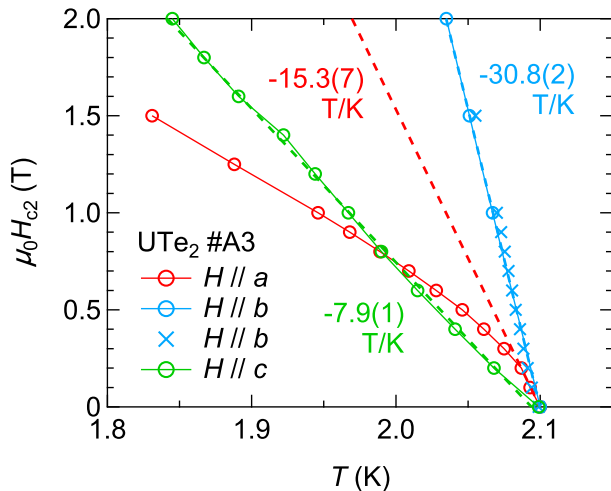
FIG. 4. Upper critical field in the low-field region with the magnetic field along the *a* axis (red), *b* axis (blue), and *c* axis (green) in crystal #A3. The data are obtained by specific-heat measurements on a high-quality crystal with $T_c = 2.1$ K. The broken lines are the initial slopes obtained by the linear fitting of the data near T_c. The errors shown in the slope values are estimated from the standard deviation of the linear fitting.

the experimental critical fields (H_c, H_{c1}, and H_{c2}) along the *a* axis satisfy the usual thermodynamic relations of Eqs. (3) and (4). This result suggests that the significant change in the slope of H_{c2}^a near T_c shown in Fig. 4 is an intrinsic property of UTe$_2$ possibly induced by the reduction of ferromagnetic fluctuations with $H \parallel a$ [8]. In the previous study, because the critical fields violated the above GL relations, the authors assumed a magnetic field effect on T_c, dT_c/dH [36]. However, our results consistent with the GL relations for $H \parallel a$ indicate that the dT_c/dH effect is negligible as long as we focus on the initial slopes of the critical fields.

In contrast to H_{c1}^a, however, the initial slope of H_{c1}^b is significantly larger than the expected H_{c1}^{cal} value. In addition to the steep initial slope, H_{c1}^b and H_{c1}^c in ultraclean UTe$_2$ show an unusual increase below 0.5 K, which has not been observed previously. A similar $H_{c1}(T)$ behavior was reported in multiband iron-based superconductors [39,40] and the chiral superconductor candidates, UPt$_3$ [41,42] and PrOs$_4$Sb$_{12}$ [43]. We emphasize that the increase of $H_{c1}(T)$ at low temperatures in these materials was observed regardless of the magnetic-field directions, which is clearly different from the case in UTe$_2$ where the increase is discernible only in $H \parallel b$ and $H \parallel c$. Moreover, magnetic penetration depth measurements in PrOs$_4$Sb$_{12}$ also show a kink at lower temperatures [44], while the anisotropic penetration depth in UTe$_2$ shows smooth T dependence around 0.5 K [13]. Thus, while the enhancement of H_{c1} at low temperatures in the previous studies on the various superconductors reflects the increase of superfluid density, the anomalous $H_{c1}(T)$ in UTe$_2$ likely has a different origin which induces a large anisotropy.

Because the H_{c1} value is determined by the vortex line energy, the unusual $H_{c1}^b(T)$ and $H_{c1}^c(T)$ behaviors can be

related to an exotic vortex state. As for the vortices in UTe$_2$, recent scanning superconducting quantum interference device measurements on the (011) plane observed pinned vortices and antivortices even in a zero-field cooling condition, which can be related to the presence of strong and slow magnetic fluctuations detected in μSR and NMR studies [45]. Moreover, optical Kerr effect measurements on the (001) plane suggest the presence of magnetized vortices induced by strong magnetic fluctuations. From these results, we consider that the enhancement of $H_{c1}^b(T)$ and $H_{c1}^c(T)$ is related to the strong Ising-like ferromagnetic fluctuations along the *a* axis inducing an exotic vortex state in UTe$_2$. We note that anomalous low-T behavior has been also detected in $1/T_1T$ of NMR measurements [46] and zero-field relaxation rate of μSR measurements [17,47].

The relationship between strong magnetic fluctuations and the enhancement in H_{c1} has been investigated in BaFe$_2$(As$_{1-x}$P$_x$)$_2$ [34]. In this system, an antiferromagnetic quantum critical point (QCP) appears at $x = 0.3$ where $\lambda(0)$ shows a sharp peak reflecting the strong mass enhancement [48]. In contrast, H_{c1} also shows a peak at QCP, contradicting the expected behavior from Eq. (2). This discrepancy suggests that the vortex-line energy is significantly enhanced by the strong magnetic fluctuations near QCP. Thus, considering the presence of strong anisotropic ferromagnetic fluctuations in UTe$_2$, the vortex-line energy can be anisotropically enhanced by the Ising-like magnetic fluctuations. Indeed, the normal-state NMR measurements in UTe$_2$ [16] reported that $1/T_1T$ shows a pronounced low-T enhancement for $H \parallel b$ and $H \parallel c$, which is absent for $H \parallel a$. This shows a good correspondence with the anisotropic H_{c1} enhancement.

In conclusion, we measured the critical fields, $H_c(T)$, $H_{c1}(T)$, and $H_{c2}(T)$, in high-quality single crystals of UTe$_2$ with $T_c = 2.1$ K. While the three critical fields for $H \parallel a$ satisfy the usual GL relations near T_c, the experimental H_{c1}^b and H_{c1}^c are larger than the expected values, which become more apparent below 0.5 K. These results indicate that the anisotropic ferromagnetic fluctuations in UTe$_2$ significantly enhance the vortex-line energy with $H \parallel b$ and $H \parallel c$. Our experimental results not only suggest that an exotic vortex state caused by anisotropic ferromagnetic fluctuations is realized in UTe$_2$, but also promote further studies on magnetic fluctuations in high-quality single crystals of UTe$_2$ with low magnetic impurity density.

[1] S. Ran, C. Eckberg, Q.-P. Ding, Y. Furukawa, T. Metz, S. R. Saha, I.-L. Liu, M. Zic, H. Kim, J. Paglione, and N. P. Butch, Nearly ferromagnetic spin-triplet superconductivity, Science **365**, 684 (2019).

[2] D. Aoki, J.-P. Brison, J. Flouquet, K. Ishida, G. Knebel, Y. Tokunaga, and Y. Yanase, Unconventional superconductivity in UTe$_2$, J. Phys.: Condens. Matter **34**, 243002 (2022).

[3] S. Ran, I.-L. Liu, Y. S. Eo, D. J. Campbell, P. M. Neves, W. T. Fuhrman, S. R. Saha, C. Eckberg, H. Kim, D. Graf, F. Balakirev, J. Singleton, J. Paglione, and N. P. Butch, Extreme magnetic field-boosted superconductivity, Nat. Phys. **15**, 1250 (2019).

[4] D. Braithwaite, M. Vališka, G. Knebel, G. Lapertot, J.-P. Brison, A. Pourret, M. E. Zhitomirsky, J. Flouquet, F. Honda, and D. Aoki, Multiple superconducting phases in a nearly ferromagnetic system, Commun. Phys. **2**, 147 (2019).

[5] S. M. Thomas, F. B. Santos, M. H. Christensen, T. Asaba, F. Ronning, J. D. Thompson, E. D. Bauer, R. M. Fernandes, G. Fabbris, and P. F. S. Rosa, Evidence for a pressure-induced antiferromagnetic quantum critical point in intermediate-valence UTe$_2$, Sci. Adv. **6**, eabc8709 (2020).

[6] D. Aoki, F. Honda, G. Knebel, D. Braithwaite, A. Nakamura, D. Li, Y. Homma, Y. Shimizu, Y. J. Sato, J.-P. Brison, and J. Flouquet, Multiple superconducting phases and unusual enhancement of the upper critical field in UTe$_2$, J. Phys. Soc. Jpn. **89**, 053705 (2020).

[7] K. Kinjo, H. Fujibayashi, S. Kitagawa, K. Ishida, Y. Tokunaga, H. Sakai, S. Kambe, A. Nakamura, Y. Shimizu, Y. Homma, D. X. Li, F. Honda, D. Aoki, K. Hiraki, M. Kimata, and T. Sasaki, Magnetic field-induced transition with spin rotation in the superconducting phase of UTe$_2$, Phys. Rev. B **107**, L060502 (2023).

[8] A. Rosuel, C. Marcenat, G. Knebel, T. Klein, A. Pourret, N. Marquardt, Q. Niu, S. Rousseau, A. Demuer, G. Seyfarth, G. Lapertot, D. Aoki, D. Braithwaite, J. Flouquet, and J.-P. Brison, Field-Induced Tuning of the Pairing State in a Superconductor, Phys. Rev. X **13**, 011022 (2023).

[9] H. Sakai, Y. Tokiwa, P. Opletal, M. Kimata, S. Awaji, T. Sasaki, D. Aoki, S. Kambe, Y. Tokunaga, and Y. Haga, Field induced multiple superconducting phases in UTe$_2$ along hard magnetic axis, arXiv:2210.05909.

[10] L. Jiao, S. Howard, S. Ran, Z. Wang, J. O. Rodriguez, M. Sigrist, Z. Wang, N. P. Butch, and V. Madhavan, Chiral superconductivity in heavy-fermion metal UTe$_2$, Nature (London) **579**, 523 (2020).

[11] I. M. Hayes, D. S. Wei, T. Metz, J. Zhang, Y. S. Eo, S. Ran, S. R. Saha, J. Collini, N. P. Butch, D. F. Agterberg, A. Kapitulnik, and J. Paglione, Multicomponent superconducting order parameter in UTe$_2$, Science **373**, 797 (2021).

[12] S. Bae, H. Kim, Y. S. Eo, S. Ran, I.-l. Liu, W. T. Fuhrman, J. Paglione, N. P. Butch, and S. M. Anlage, Anomalous normal fluid response in a chiral superconductor UTe$_2$, Nat. Commun. **12**, 2644 (2021).

[13] K. Ishihara, M. Roppongi, M. Kobayashi, Y. Mizukami, H. Sakai, Y. Haga, K. Hashimoto, and T. Shibauchi, Chiral superconductivity in UTe$_2$ probed by anisotropic low-energy excitations, arXiv:2105.13721.

[14] G. Knebel, W. Knafo, A. Pourret, Q. Niu, M. Vališka, D. Braithwaite, G. Lapertot, M. Nardone, A. Zitouni, S. Mishra, I. Sheikin, G. Seyfarth, J.-P. Brison, D. Aoki, and J. Flouquet, Field-reentrant superconductivity close to a metamagnetic transition in the heavy-fermion superconductor UTe$_2$, J. Phys. Soc. Jpn. **88**, 063707 (2019).

[15] D. Aoki, K. Ishida, and J. Flouquet, Review of U-based ferromagnetic superconductors: Comparison between UGe$_2$, URhGe, and UCoGe, J. Phys. Soc. Jpn. **88**, 022001 (2019).

[16] Y. Tokunaga, H. Sakai, S. Kambe, T. Hattori, N. Higa, G. Nakamine, S. Kitagawa, K. Ishida, A. Nakamura, Y. Shimizu, Y. Homma, D. Li, F. Honda, and D. Aoki, ^{125}Te-NMR study on a single crystal of heavy fermion superconductor UTe$_2$, J. Phys. Soc. Jpn. **88**, 073701 (2019).

[17] S. Sundar, S. Gheidi, K. Akintola, A. M. Côté, S. R. Dunsiger, S. Ran, N. P. Butch, S. R. Saha, J. Paglione, and J. E. Sonier, Coexistence of ferromagnetic fluctuations and superconductivity in the actinide superconductor UTe$_2$, Phys. Rev. B **100**, 140502(R) (2019).

[18] Y. Tokunaga, H. Sakai, S. Kambe, Y. Haga, Y. Tokiwa, P. Opletal, H. Fujibayashi, K. Kinjo, S. Kitagawa, K. Ishida, A. Nakamura, Y. Shimizu, Y. Homma, D. Li, F. Honda, and D. Aoki, Slow electronic dynamics in the paramagnetic state of UTe$_2$, J. Phys. Soc. Jpn. **91**, 023707 (2022).

[19] C. Duan, K. Sasmal, M. B. Maple, A. Podlesnyak, J.-X. Zhu, Q. Si, and P. Dai, Incommensurate Spin Fluctuations in the Spin-Triplet Superconductor Candidate UTe$_2$, Phys. Rev. Lett. **125**, 237003 (2020).

[20] W. Knafo, G. Knebel, P. Steffens, K. Kaneko, A. Rosuel, J.-P. Brison, J. Flouquet, D. Aoki, G. Lapertot, and S. Raymond, Low-dimensional antiferromagnetic fluctuations in the heavy-fermion paramagnetic ladder compound UTe$_2$, Phys. Rev. B **104**, L100409 (2021).

[21] C. Duan, R. E. Baumbach, A. Podlesnyak, Y. Deng, C. Moir, A. J. Breindel, M. B. Maple, E. M. Nica, Q. Si, and P. Dai, Resonance from antiferromagnetic spin fluctuations for superconductivity in UTe$_2$, Nature (London) **600**, 636 (2021).

[22] N. P. Butch, S. Ran, S. R. Saha, P. M. Neves, M. P. Zic, J. Paglione, S. Gladchenko, Q. Ye, and J. A. Rodriguez-Rivera, Symmetry of magnetic correlations in spin-triplet superconductor UTe$_2$, npj Quantum Mater. **7**, 39 (2022).

[23] S. M. Thomas, C. Stevens, F. B. Santos, S. S. Fender, E. D. Bauer, F. Ronning, J. D. Thompson, A. Huxley, and P. F. S. Rosa, Spatially inhomogeneous superconductivity in UTe$_2$, Phys. Rev. B **104**, 224501 (2021).

[24] P. F. S. Rosa, A. Weiland, S. S. Fender, B. L. Scott, F. Ronning, J. D. Thompson, E. D. Bauer, and S. M. Thomas, Single thermodynamic transition at 2 K in superconducting UTe$_2$ single crystals, Commun. Mater. **3**, 33 (2022).

[25] W. Knafo, M. Nardone, M. Vališka, A. Zitouni, G. Lapertot, D. Aoki, G. Knebel, and D. Braithwaite, Comparison of two superconducting phases induced by a magnetic field in UTe$_2$, Commun. Phys. **4**, 40 (2021).

[26] Y. Haga, P. Opletal, Y. Tokiwa, E. Yamamoto, Y. Tokunaga, S. Kambe, and H. Sakai, Effect of uranium deficiency on normal and superconducting properties in unconventional superconductor UTe$_2$, J. Phys.: Condens. Matter **34**, 175601 (2022).

[27] H. Sakai, P. Opletal, Y. Tokiwa, E. Yamamoto, Y. Tokunaga, S. Kambe, and Y. Haga, Single crystal growth of superconducting UTe$_2$ by molten salt flux method, Phys. Rev. Mater. **6**, 073401 (2022).

[28] Y. Tokiwa, P. Opletal, H. Sakai, K. Kubo, E. Yamamoto, S. Kambe, M. Kimata, S. Awaji, T. Sasaki, D. Aoki, Y. Tokunaga, and Y. Haga, Stabilization of superconductivity

by metamagnetism in an easy-axis magnetic field on UTe$_2$, arXiv:2210.11769.

[29] D. Aoki, H. Sakai, P. Opletal, Y. Tokiwa, J. Ishizuka, Y. Yanase, H. Harima, A. Nakamura, D. Li, Y. Homma, Y. Shimizu, G. Knebel, J. Flouquet, and Y. Haga, First observation of the de Haas-van Alphen effect and Fermi surfaces in the unconventional superconductor UTe$_2$, J. Phys. Soc. Jpn. **91**, 083704 (2022).

[30] O. Tanaka, Y. Mizukami, R. Harasawa, K. Hashimoto, K. Hwang, N. Kurita, H. Tanaka, S. Fujimoto, Y. Matsuda, E.-G. Moon, and T. Shibauchi, Thermodynamic evidence for a field-angle-dependent Majorana gap in a Kitaev spin liquid, Nat. Phys. **18**, 429 (2022).

[31] T. Shibauchi, M. Konczykowski, C. J. van der Beek, R. Okazaki, Y. Matsuda, J. Yamaura, Y. Nagao, and Z. Hiroi, Vortex Redistribution Below the First-Order Transition Temperature in the β-Pyrochlore Superconductor KOs$_2$O$_6$, Phys. Rev. Lett. **99**, 257001 (2007).

[32] R. Okazaki, M. Konczykowski, C. J. van der Beek, T. Kato, K. Hashimoto, M. Shimozawa, H. Shishido, M. Yamashita, M. Ishikado, H. Kito, A. Iyo, H. Eisaki, S. Shamoto, T. Shibauchi, and Y. Matsuda, Lower critical fields of superconducting PrFeAsO$_{1-y}$ single crystals, Phys. Rev. B **79**, 064520 (2009).

[33] R. Okazaki, M. Shimozawa, H. Shishido, M. Konczykowski, Y. Haga, T. D. Matsuda, E. Yamamoto, Y. Onuki, Y. Yanase, T. Shibauchi, and Y. Matsuda, Anomalous temperature dependence of lower critical field in ultraclean URu$_2$Si$_2$, J. Phys. Soc. Jpn. **79**, 084705 (2010).

[34] C. Putzke, P. Walmsley, J. D. Fletcher, L. Malone, D. Vignolles, C. Proust, S. Badoux, P. See, H. E. Beere, D. A. Ritchie, S. Kasahara, Y. Mizukami, T. Shibauchi, Y. Matsuda, and A. Carrington, Anomalous critical fields in quantum critical superconductors, Nat. Commun. **5**, 5679 (2014).

[35] See Supplemental Material at http://link.aps.org/supplemental/10.1103/PhysRevResearch.5.L022002 for the detailed calculations of H_c, the position dependence of the magnetic induction, and the analysis to obtain the H_p values.

[36] C. Paulsen, G. Knebel, G. Lapertot, D. Braithwaite, A. Pourret, D. Aoki, F. Hardy, J. Flouquet, and J.-P. Brison, Anomalous anisotropy of the lower critical field and Meissner effect in UTe$_2$, Phys. Rev. B **103**, L180501 (2021).

[37] E. H. Brandt, Irreversible magnetization of pin-free type-II superconductors, Phys. Rev. B **60**, 11939 (1999).

[38] S. Kittaka, Y. Shimizu, T. Sakakibara, A. Nakamura, D. Li, Y. Homma, F. Honda, D. Aoki, and K. Machida, Orientation

of point nodes and nonunitary triplet pairing tuned by the easy-axis magnetization in UTe$_2$, Phys. Rev. Res. **2**, 032014(R) (2020).

[39] Y. J. Song, J. S. Ghim, J. H. Yoon, K. J. Lee, M. H. Jung, H.-S. Ji, J. H. Shim, Y. Bang, and Y. S. Kwon, Small anisotropy of the lower critical field and the $s_\pm$-wave two-gap feature in single-crystal LiFeAs, Europhys. Lett. **94**, 57008 (2011).

[40] A. Adamski, C. Krellner, and M. Abdel-Hafiez, Signature of multigap nodeless superconductivity in fluorine-doped Nd-FeAsO, Phys. Rev. B **96**, 100503(R) (2017).

[41] E. Vincent, J. Hammann, L. Taillefer, K. Behnia, N. Keller, and J. Flouquet, Low-field diamagnetic response of the superconducting phases in UPt$_3$, J. Phys.: Condens. Matter **3**, 3517 (1991).

[42] A. Amann, A. C. Mota, M. B. Maple, and H. von Löhneysen, Magnetic properties of UPt$_3$ in the superconducting state, Phys. Rev. B **57**, 3640 (1998).

[43] J. Juraszek, R. Wawryk, Z. Henkie, M. Konczykowski, and T. Cichorek, Symmetry of Order Parameters in Multiband Superconductors LaRu$_4$As$_{12}$ and PrOs$_4$Sb$_{12}$ Probed by Local Magnetization Measurements, Phys. Rev. Lett. **124**, 027001 (2020).

[44] E. E. M. Chia, M. B. Salamon, H. Sugawara, and H. Sato, Probing the Superconducting Gap Symmetry of PrOs$_4$Sb$_{12}$: A Penetration Depth Study, Phys. Rev. Lett. **91**, 247003 (2003).

[45] Y. Iguchi, H. Man, S. M. Thomas, F. Ronning, P. F. S. Rosa, and K. A. Moler, Microscopic imaging homogeneous and single phase superfluid density in UTe$_2$, arXiv:2210.09562.

[46] G. Nakamine, S. Kitagawa, K. Ishida, Y. Tokunaga, H. Sakai, S. Kambe, A. Nakamura, Y. Shimizu, Y. Homma, D. Li, F. Honda, and D. Aoki, Superconducting properties of heavy fermion UTe$_2$ revealed by ^{125}Te-nuclear magnetic resonance, J. Phys. Soc. Jpn. **88**, 113703 (2019).

[47] S. Sundar, N. Azari, M. Goeks, S. Gheidi, M. Abedi, M. Yakovlev, S. R. Dunsiger, J. M. Wilkinson, S. J. Blundell, T. E. Metz, I. M. Hayes, S. R. Saha, S. Lee, A. J. Woods, R. Movshovich, S. M. Thomas, P. F. S. Rosa, N. P. Butch, J. Paglione, and J. E. Sonier, Ubiquitous spin freezing in the superconducting state of UTe$_2$, Commun. Phys. **6**, 24 (2023).

[48] K. Hashimoto, K. Cho, T. Shibauchi, S. Kasahara, Y. Mizukami, R. Katsumata, Y. Tsuruhara, T. Terashima, H. Ikeda, M. A. Tanatar, H. Kitano, N. Salovich, R. W. Giannetta, P. Walmsley, A. Carrington, R. Prozorov, and Y. Matsuda, A sharp peak of the zero-temperature penetration depth at optimal composition in BaFe$_2$(As$_{1-x}$P$_x$)$_2$, Science **336**, 1554 (2012).